

# Wave Energy Assessment Along the Moroccan Atlantic Coast

Hafsa Bouhrim<sup>1</sup> · Abdellatif El Marjani<sup>1</sup>

Received: 29 January 2018 / Accepted: 13 June 2018 / Published online: 7 December 2018  
© Harbin Engineering University and Springer-Verlag GmbH Germany, part of Springer Nature 2019

## Abstract

The aim of the present work is to assess the offshore wave energy potential along the Atlantic coast of Morocco. Research works of this paper focus on the identification of the most energetic sites for wave energy converters (WECs) deployment. For this purpose, 11 sites have been explored; all of them are located at more than 40m depth on the Moroccan Atlantic coast. The wave power at each site is computed on the basis of wave data records in terms of significant wave height and energy period provided by the Wave Watch three (WW3) model. Results indicate that the coast sites located between latitudes 30° 30' N and 33° N are the most energetic with an annual average wave power estimated at about  $30 \text{ kW} \cdot \text{m}^{-1}$ , whereas, in the other sites, the wave power is significantly lower. Moreover, the study of the monthly and seasonal temporal variability is found to be uniform in the powerful sites with values four times greater in winter than in summer. The directional investigation on the significant wave height has shown that for almost all the powerful sites, the incoming waves have a dominant sector ranging between Northern (N) and Western-Northern-Western (WNW) directions.

**Keywords** Wave energy · Moroccan Atlantic coast · Wave energy converter (WEC) · Wave Watch 3 (WW3) · Seasonal and temporal variability · Directional wave height investigation · Power roses · Occurrence bivariate distributions

## 1 Introduction

With the increasing demand in terms of energy, new resources are needed to satisfy the requirements of the world's population and industries. Within this context, the possibility of producing electrical energy from marine renewable resources (Lewis et al. 2011), in particular from the wave energy, has been intensively investigated during the last decades.

It has been established that the highest energy ocean waves are concentrated at higher latitudes, greater than 40° from the equator with a high power level around  $70 \text{ kW} \cdot \text{m}^{-1}$  as depicted in Fig. 1. According to the same figure, it can be noted that the higher is the altitude, the higher is the power level. While Morocco has a lengthy Atlantic coastline spanned on 3000 km, the global offshore wave energy is estimated at nearly 90 000 MW (Mørk et al. 2010) which is 15 times its wind potential. This makes the country able to reinforce significantly its policy in terms of increasing the exploitation of its renewable energy resources. More than 90% of energy

needs in Morocco are satisfied by means of external importation (Aparicio 2014). Thus, exploiting new energetic resources will contribute to reducing its energetic dependency.

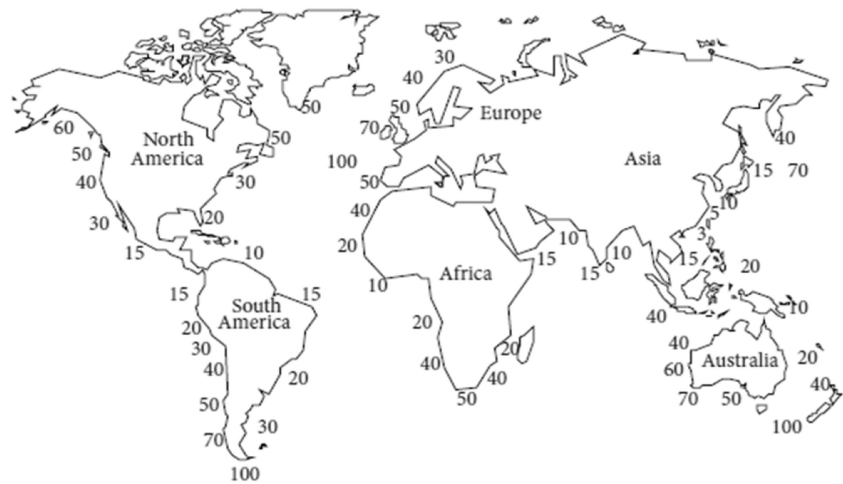
In comparison with other renewable energy sources (solar and wind energies), the global wave energy potential is expected to be of the same order of magnitude of the world electrical energy consumption (Angelis-Dimakakis et al. 2010). Furthermore, exploiting waves as a resource of renewable energy presents significant advantages over other alternative renewable energy techniques as listed below:

- Waves can propagate for large distances with little energy loss, as in (Drew et al. 2009; López et al. 2013) the storms taking their origins from the western side of the Atlantic Ocean propagate with little energy loss to the western coast of Europe;
- Ocean waves are of greater energy density compared with the other renewable energy sources (Drew et al. 2009);
- The seasonal variability of wave energy follows the demand in terms of electricity in intermediate climates;
- Wave energy converters do not generate greenhouse gases (GHGs) when operating and have a low lifecycle;
- Wave power production a day is continuously estimated to 90% of the time, while solar and wind devices generate a power of only 20% to 30% a time (Fadaeenejad et al. 2014).

✉ Abdellatif El Marjani  
elmarjani@emi.ac.ma

<sup>1</sup> EMISys Team Research, E3S Research Center, Turbomachinery Lab, Mohammadia School of Engineers, Mohammed V University in Rabat, Avenue Ibn Sina, Agdal, BP 765, Rabat, Morocco

**Fig. 1** Offshore world annual mean wave power distribution per unit crest length ( $\text{kW} \cdot \text{m}^{-1}$ ) (Joubert 2008)



However, to be able to harness energy from waves, a number of challenges need to be tackled to successfully meet the commercial competitiveness in the global energy market. They include the following:

- Wave direction in offshore areas varies highly; hence, wave energy systems must be adapted to these variations to capture as much energy as possible. Near the shore, the wave directions are identified in advance (Drew et al. 2009);
- The major challenge is to convert the slow (frequency 0.1 Hz), random, and oscillatory motion of waves into useful motion to drive a generator with an output quality acceptable to the utility network (Drew et al. 2009);
- Sea waves vary in terms of period and height, so does the corresponding power level. This variable energy has to be converted into a smooth electrical signal; therefore, to provide regular power outputs energy storage systems is recommended (Drew et al. 2009; López et al. 2013).

The present paper is organized as follows: Section 2 presents a brief outline of the technologies used for wave energy conversion. In Section 3, the studied sites are presented, as well as the methodology of their wave energy potential assessment. Section 4 presents the results and discussions on the sites with the highest energy potential, the seasonal and

monthly variations of wave energy, and the suitable zones for WECs deployment. Finally, a conclusion is drawn in Section 5.

## 2 Wave Energy Conversion

Nowadays, a wide variety of wave energy conversion systems have been developed for electrical power production (López et al. 2013; Antonio and Falcão 2014). These wave energy converters are generally classified, according to their locations (near-shore, offshore, and shoreline) and working principle as described in the following sections.

### 2.1 Location

According to their location with respect to the sea coastline, the WECs can be categorized as follows (Fig. 2):

- Offshore devices are generally submerged or floating structures located far from the shore in deep waters exceeding 40 m (Duckers 2004). Being placed in the open seas, these devices may absorb abundant amounts of wave energy. However, this, also, has disadvantages: the structure has to bear high loads in addition to the problem of survivability (i.e., difficulties to maintain and construct).
- Near-shore devices are installed in relatively moderate water depths ranging between 10 and 25 m, or less than one quarter of the wavelength (Duckers 2004). These converters are usually fixed to the sea bottom to be able to avoid moorings and to harvest the maximum wave energy.
- Shoreline devices are mounted on or next to the shore (Fig. 3) and can be allocated in shallow waters. Being near to the coast, these converters are easy to maintain and install. However, the waves at the shoreline contain less energy due to their interaction with the sea bottom (Antonio and Falcão 2010).

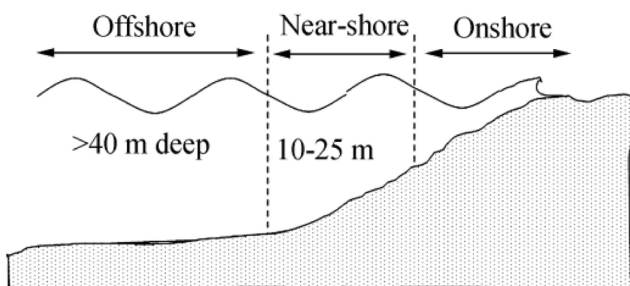


**Fig. 2** Locations of WECs

**Fig. 3** Onshore wave energy converters around the world (Falcão and Henriques 2016)



## 2.2 Working Principle

According to their working principle, the WECs can be categorized as follows:

- Differential pressure devices are submerged point absorbers placed near shore and attached to the seabed by a single point, they use the pressure difference generated between the crest and the trough of the wave to create an up and down motion of the device. An example of these devices is the Archimedes Wave Swing AWS Ocean (250 kW) (Fig. 4c).
- Oscillating water columns (OWCs): consist of a submerged air chamber connected to the atmosphere by means of a circular duct inside which a bidirectional flow turbine is installed. The flow rate of air through the turbine is generated by the successive incident sea water waves that compress and depressurize air in the air chamber by means of the periodic motion of the oscillating free surface (Fadaeenejad et al. 2014). Examples of these systems are Oceanlinx (AU) (Fig. 5a) and Ocean Energy OE Buoy (IRL) (Fig. 4a).
- Floating structures: floating structures moved by the oscillatory motion of the waves. This motion may be either horizontal, vertical, or pitch. As a type of devices, Ocean Power Technologies OPT (USA) (Fig. 4e) and Searaser (UK) (Fig. 5d).
- Overtopping devices: can be placed onshore or floating offshore, they capture the incident wave and fill a reservoir above the sea level, which causes an increase in water pressure. This water is then released back to the ocean due to gravity through the turbines. An example of such devices is the Sea Slot-cone Generator SSG wave energy converter (150 kW) (Fig. 3c), Wave Dragon (DK) (Fig. 4d), and OE Buoy (IRL) (Fig. 4a).

## 3 Moroccan Atlantic Coast Wave Energy

A number of research studies in the field of wave energy have been carried out using spectral wave models as reliable tools to assess and forecast the coastal wave resources around the globe (Arinaga and Cheung 2012; Cornett 2008). For

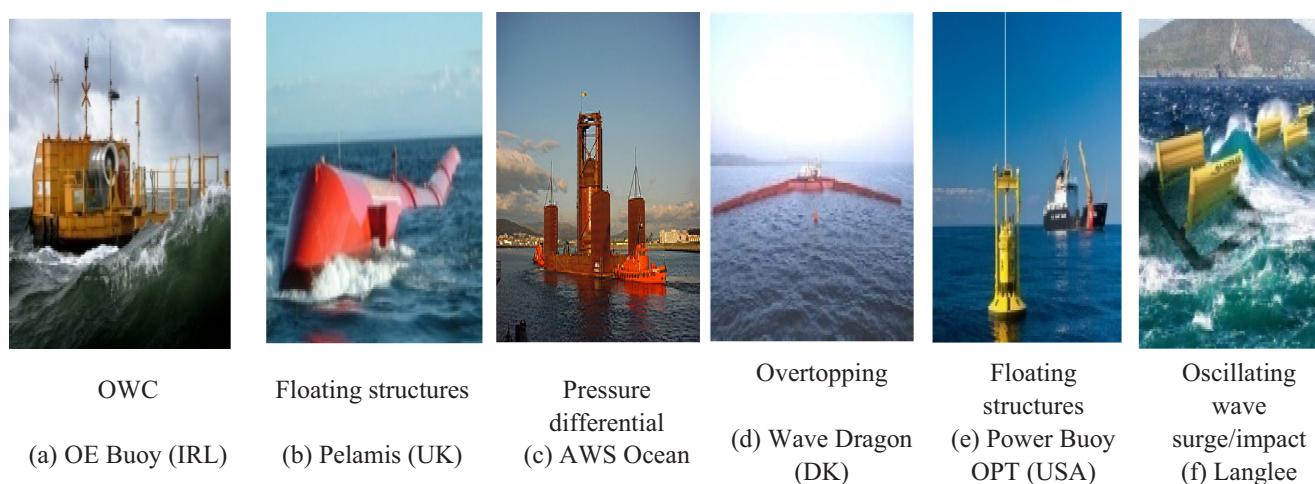


**Fig. 4** Offshore wave energy converters around the world (Antonio and Falcão 2010)

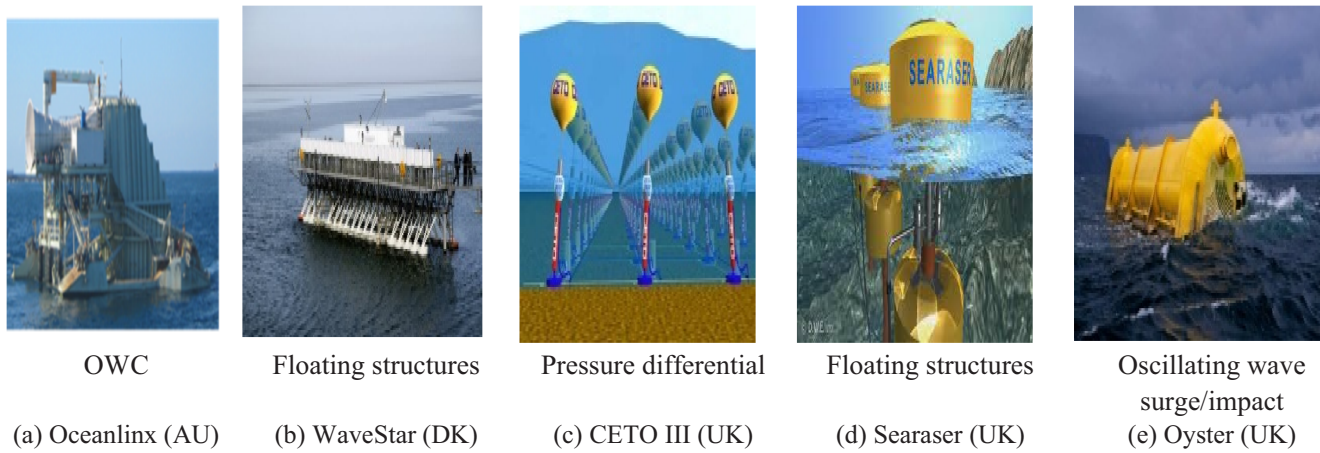


**Fig. 5** Near-shore wave energy converters around the world (Antonio and Falcão 2010)

instance, Sierra et al. (2016) utilized the third-generation spectral model WAM (Wave Model) (Hasselmann et al. 1988) to analyze the wave energy potential along the Atlantic coast of Morocco, while in the present work, the WW3 spectral wave model has been exploited. Results obtained by these authors give a detailed analysis of wave energy potential for a significant number of sites. Results obtained by these authors give a detailed wave energy potential for a significant number of sites. However, no information about sites on the Southern

Atlantic coast of Morocco is provided. For this, the present potential assessment has been extended to this region. Furthermore, in order to identify the sea state that comprises significant wave power, the bivariate distributions of occurrences should be determined. Zodiatis et al. (2014) used the same model to produce 10-year database for the wave energy potential in the Eastern Mediterranean Levantine Basin. Vannucchi et al. (2012) and Holmbom (2011) investigate wave and current energies by using the Mike 21 software for

**Fig. 6** Moroccan map with the locations of the 11 sites

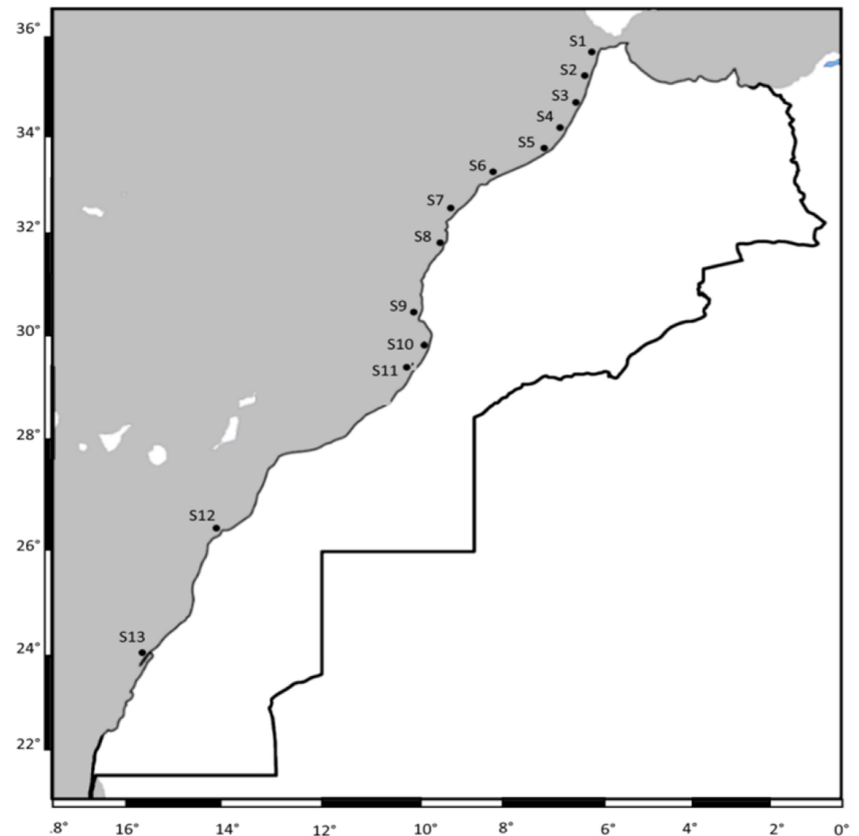




**Table 1** Geographical coordinates of the 11 sites

| Sites    | Longitudes (W) | Latitudes (N) | Depths/m |
|----------|----------------|---------------|----------|
| $S_1$    | 6° 04'         | 35° 46'       | 60       |
| $S_2$    | 6° 20'         | 35° 30'       | 110      |
| $S_3$    | 6° 30'         | 35° 11'       | 130      |
| $S_4$    | 7° 09'         | 33° 47'       | 200      |
| $S_5$    | 7° 02'         | 33° 50'       | 140      |
| $S_6$    | 8° 30'         | 33° 30'       | 60       |
| $S_7$    | 8° 30'         | 33° 15'       | 90       |
| $S_8$    | 9° 30'         | 32° 30'       | 60       |
| $S_9$    | 9° 35'         | 30° 25'       | 120      |
| $S_{10}$ | 10° 00'        | 30° 00'       | 125      |
| $S_{11}$ | 10° 10'        | 29° 22'       | 60       |
| $S_{12}$ | 26° 11'        | 14° 38'       | 70       |
| $S_{13}$ | 23° 70'        | 15° 94'       | 80       |

the Mediterranean and Baltic seas, respectively. Other studies employed the wave model SWAN (Simulating Waves Nearshore) (Booij et al. 1999), as in the Persian Gulf to produce wave data parameters and determine wave energy variations over 25 years (Kamranzad et al. 2013). In addition, this tool has been used in Spain to assess the wave energy potential along the Death Coast (Iglesias and Carballo 2009), in the Mediterranean Sea (Liberti et al. 2013; Iuppa et al. 2015), and finally, in the south coasts of the black sea over a period of 14 years (Akpınar and Kömürçü 2012).

Gonçalves et al. (2014) utilized recently both WW3 which is developed by Tolman et al. (2002) and SWAN for wave generation along the Atlantic Basin and the identification of wave transformation in the Canary Islands; the two models are also combined in an assessment study of the wave energy resources along the Hawaiian Islands (Stopa et al. 2013).

### 3.1 Study Area

Morocco is located in the northern region of Africa between latitudes 21° to 36° N and longitudes 1° to 17° W, bordering Mauritania to the southeast and Algeria to the east Fig. 6. In

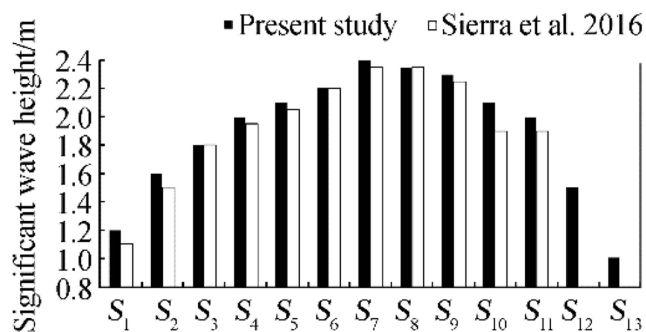


**Fig. 7** Comparison of the significant wave height ( $H_s$ ) with results of Sierra et al. (2016)

this paper, the area of interest is the Atlantic coast of Morocco that is spanned on about 3000 km of coastline. According to Pinet (2006), the incoming waves to the study area take their origins from the Azores Islands, where long-period swells of perpendicular direction to the coast are conducted by winds of high intensity (Gunn and Stock-Williams 2012). Moreover, the propagating wave magnitudes are reduced by both the Canary Islands from the southern area and the south-west regions of the Iberian Peninsula from the most north.

The wave energy potential and variability were assessed initially for several sites geographically distributed along the entire Atlantic coast of Morocco. However, according to the preliminary wave data analysis, 11 sites ( $S_1$  to  $S_{11}$ ) have revealed significant wave energy potential (Fig. 6) and, therefore, have been retained for a possible energy conversion with a WEC device. The geographical positions in terms of latitude, depth, and longitude of each selected location were presented in Table 1.

### 3.2 Methodology

There are several methodologies for wave energy potential assessment such as the significant wave height and period, the observed wind, and wind data using Weibull distribution (Ertekin and Yingfan 1994). One of the common methods used for wave power estimation uses the wave characteristics which are the significant wave height  $H_s$  (m) representing the average height of the highest 1/3 waves, and the energy period  $T_e$  (s) defined as the period of a single sinusoidal wave having the same energy of the sea state (Saket and Etemad-Shahid 2012; Abbaspour and Rahimi 2011). This method is used in the current study to calculate the annual mean wave power per unit crest length for deep waters which is given as a function of  $H_s$  and  $T_e$  (Iglesias et al. 2009) in Eq. (1).

$$P = \frac{\rho g^2}{64\pi} H_s^2 T_e = 0.49 H_s^2 T_e \quad (1)$$

where  $\rho$  denotes the density of the seawater ( $1025 \text{ kg} \cdot \text{m}^{-3}$ ),  $g$  is the gravitational acceleration ( $9.81 \text{ m} \cdot \text{s}^{-2}$ ).

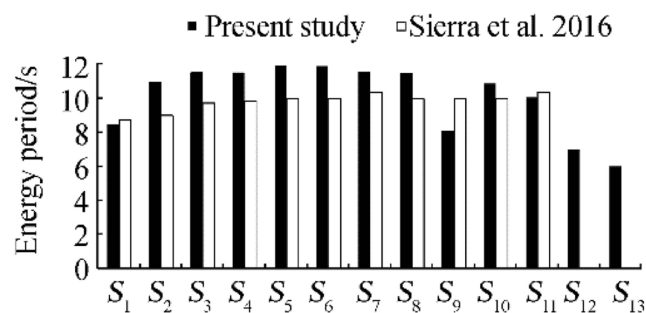


**Fig. 8** Comparison of the wave energy period ( $T_e$ ) with results of Sierra et al. (2016)

$H_s$  and  $T_e$  computation is based on the wave spectral moments:

$$T_e = \frac{m_{-1}}{m_0} \text{ and } H_s = 4m_0^{1/2} \quad (2)$$

where the  $p^{\text{th}}$  spectral moment is given by:

$$m_p = \int_0^{+\infty} f^p S(f) df \quad (3)$$

According to Table 1, almost all the 11 sites are located at depths greater than 40 m. Hence Eq. (1) can be applied in this investigation without any constraints. Moreover, since the

energy period  $T_e$  values are not available, it remains possible to estimate them using other variables as the peak period  $T_p$  given by the expression of Eq. (4) (Cornett 2008; Kamranzad et al. 2013; Sierra et al. 2013).

$$T_e = 1.14T_m \text{ and } T_p = 1.2T_m, \text{ so } T_e = 0.95T_p \quad (4)$$

where  $T_m$  is the mean period.

Thus, with Eqs. (1) and (4), the wave power per unit crest length for each site can be computed. Another factor to consider when selecting a suitable site for WEC deployment is its temporal variability (monthly and seasonal). Sites with steady

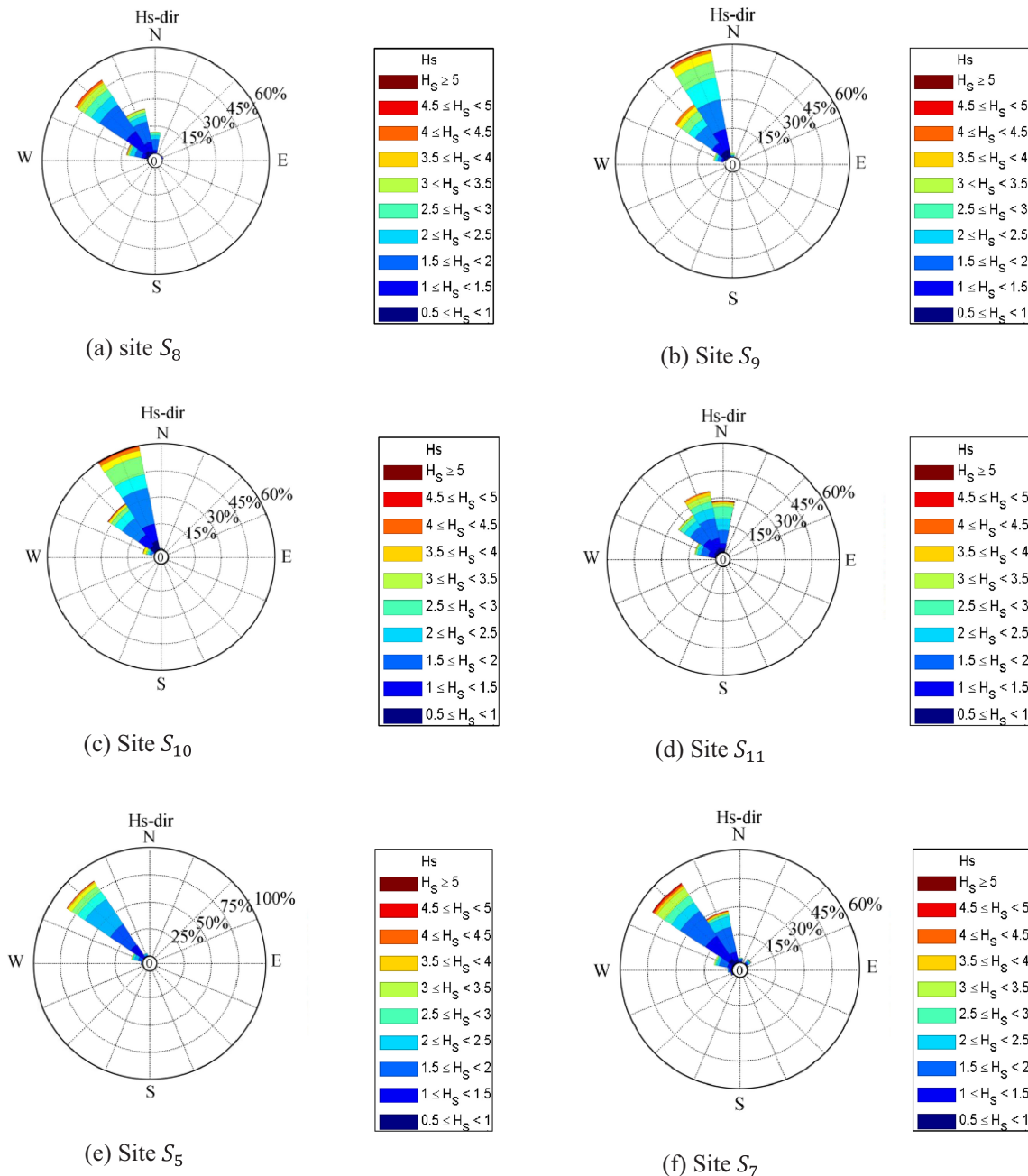


Fig. 9 Directional distribution of wave height for the most energetic sites

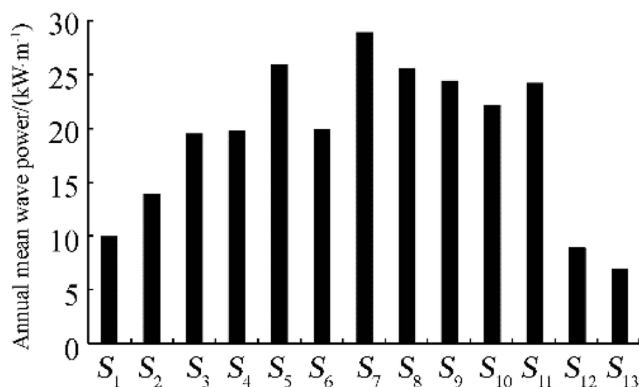


Fig. 10 The annual mean wave power at the studied sites

wave power are more attractive than those with large monthly and annual variations. In what follows, the temporal variations for the 11 sites are calculated using the following indexes (Kamranzad et al. 2013):

- The coefficient of variation  $C_v$ :

$$C_v = \frac{\sigma}{\mu} \quad (5)$$

where  $\sigma$  is the standard deviation and  $\mu$  the mean power value.

- The seasonal variability  $S_v$ :

$$S_v = \frac{P_{s.\max} - P_{s.\min}}{P_{\text{year}}} \quad (6)$$

where  $P_{s.\max}$  denotes the mean wave power for the highest-energy season,  $P_{s.\min}$  the mean wave power for the lowest-energy season, and  $P_{\text{year}}$  the annual mean wave power.

- The monthly variability  $M_v$ :

$$M_v = \frac{P_{M.\max} - P_{M.\min}}{P_{\text{year}}} \quad (7)$$

where  $P_{M.\max}$  is the mean wave power for the highest-energy month,  $P_{M.\min}$  the mean wave power for the lowest-energy month.

## 4 Results and Discussions

### 4.1 Analysis of the Wave Data Parameters

In this section, wave data parameters in terms of wave height and period variations are analyzed. Figure 7

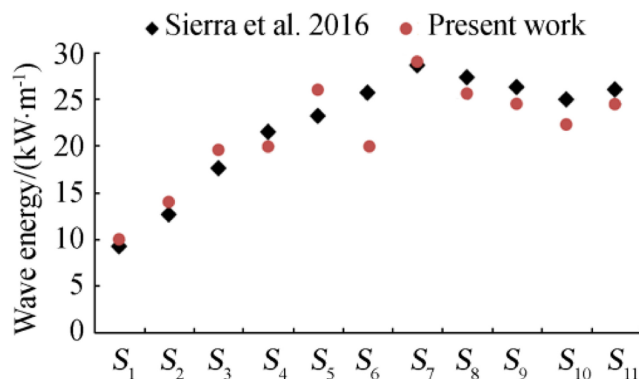


Fig. 11 Comparison of the annual mean wave power between the present work and (Sierra et al. 2016)

represents the significant wave height  $H_s$  for the 13 studied sites. It can be observed that high values of significant wave height exceeding 2 m are reached at sites  $S_7$  to  $S_9$ , with a maximal value close to 2.25 at  $S_7$ . Lower values are obtained at sites such as  $S_1$  to  $S_6$  and  $S_{12}$  to  $S_{13}$  with heights less than 1.9 m. An average value of about 2 m has been noticed for sites  $S_{10}$  and  $S_{11}$ .

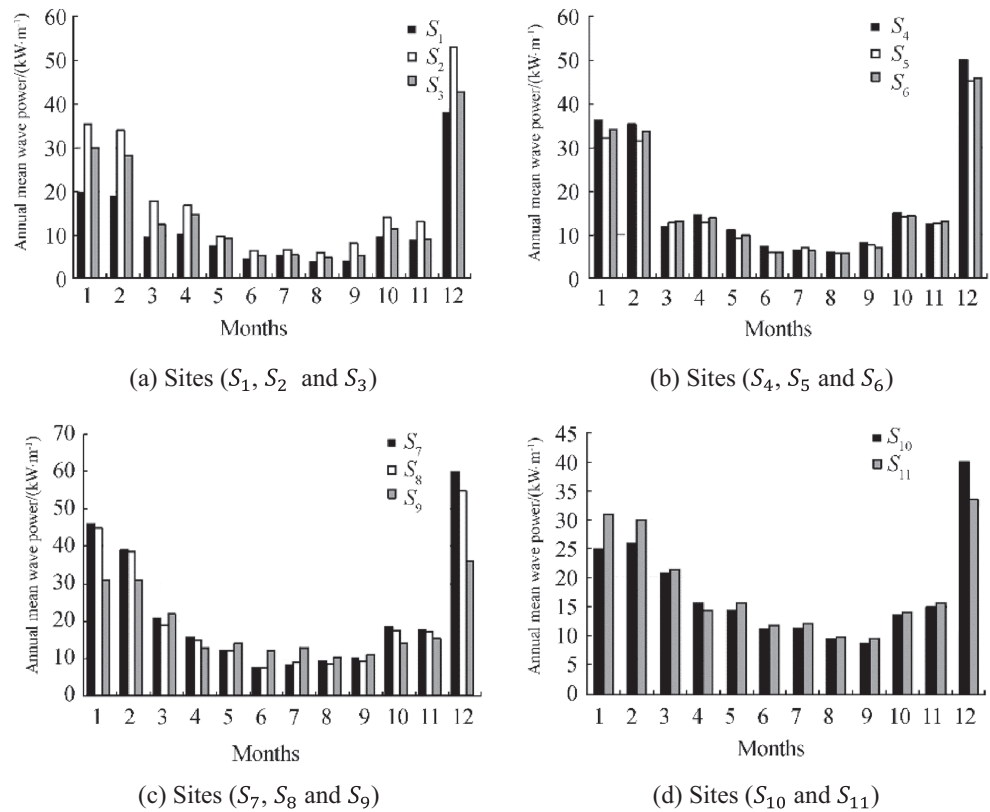
Regarding the energy period, Fig. 8 indicates that the highest mean value of 12 s is reached at  $S_5$  and  $S_6$ , followed by  $S_2$  to  $S_4$  and  $S_{10}$  with period values greater than 10 s and 11 s at  $S_8$ . The lowest value corresponds to the sites  $S_{12}$  and  $S_{13}$  with 7 s and 6 s, respectively. These values of energy period are higher, within a threshold of 10 s, in comparison with those reported by Sierra et al. (2016) as shown in Fig. 8.

Figure 9 shows the directional distribution of the significant wave height of the six powerful sites. According to these wave rose diagrams, it can be noticed that for almost all of these sites, the incoming waves have a dominant sector ranging between N and WNW. At  $S_5$ , the most energetic waves are concentrated in one direction; NW (75%) Fig. 9e. At  $S_7$ , NNW and NW directions are dominant with 29% and 50%, respectively, Fig. 9f. At  $S_9$ , the wave energy is distributed in the directions NNW (59%) and NW (35%) with a range of significant wave height of more than 4.5 m (Fig. 9b). At site  $S_{11}$ , the three dominant directions are N (29%), NNW (35%), and NW (20%) with values greater than 5 m in the North direction (Fig. 9d), and  $S_{10}$  with two dominant directions NNW (60%) and NW (35%) (Fig. 9c).

### 4.2 Annual Mean Wave Power Distribution

Figure 10 represents the spatial distribution of the average annual wave power (computed using Eq. (1)) at the studied sites. According to this figure, the most energy-rich areas are concentrated at sites  $S_7$  to  $S_9$ , with more than  $26 \text{ kW} \cdot \text{m}^{-1}$  of annual mean wave power, whereas, sites from  $S_1$  to  $S_6$  are experiencing lower values less than  $20 \text{ kW} \cdot \text{m}^{-1}$  of annual mean wave power. An average power between 20 and  $25 \text{ kW} \cdot \text{m}^{-1}$  at the locations  $S_{10}$  and  $S_{11}$ . Weak values are also

**Fig. 12** Monthly mean values of annual mean wave power per unit crest length ( $\text{kW} \cdot \text{m}^{-1}$ )



observed in the southern region at both sites  $S_{12}$  and  $S_{13}$ . The obtained results show good agreement with the results presented by Arinaga and Cheung (2012).

In addition to the spatial distribution of the wave power, it is important to analyze the temporal variability of the wave power in monthly, seasonal, and annual periods. This helps to identify the suitable sites for WECs to be allocated since locations with steady wave power are more efficient than those with large monthly and annual variations.

Referring to the results presented by Sierra et al. (2016), comparison of data from both studies has been carried out and

results are represented in Fig. 11. A correlation coefficient value of 0.924 has been obtained, which means that the computed wave power at divers regions over considerable durations is in good agreement with the results of the present study.

### 4.3 Monthly Variation in Wave Power

Figure 12 represents the average monthly wave power for the study domain. For the majority of the sites, the monthly mean wave power reaches its highest values during winter months (December to February). However, during summer months (June to August), minimal values of less than  $10 \text{ kW} \cdot \text{m}^{-1}$  are observed. At  $S_{10}$  and  $S_{11}$ , the distribution of wave power is approximately uniform (Fig. 12d).

**Table 2** Coefficient of variation

| Sites    | $C_v$ | $M_v$ | $S_v$ |
|----------|-------|-------|-------|
| $S_1$    | 1.46  | 2.88  | 1.77  |
| $S_2$    | 1.30  | 2.55  | 1.87  |
| $S_3$    | 1.40  | 2.53  | 1.70  |
| $S_4$    | 1.34  | 2.48  | 1.52  |
| $S_5$    | 1.25  | 2.4   | 1.43  |
| $S_6$    | 1.24  | 2.37  | 1.38  |
| $S_7$    | 1.23  | 1.50  | 1.34  |
| $S_8$    | 1.15  | 1.46  | 1.29  |
| $S_9$    | 0.98  | 1.40  | 1.14  |
| $S_{10}$ | 1.06  | 1.78  | 1.12  |
| $S_{11}$ | 1.05  | 1.31  | 1.10  |

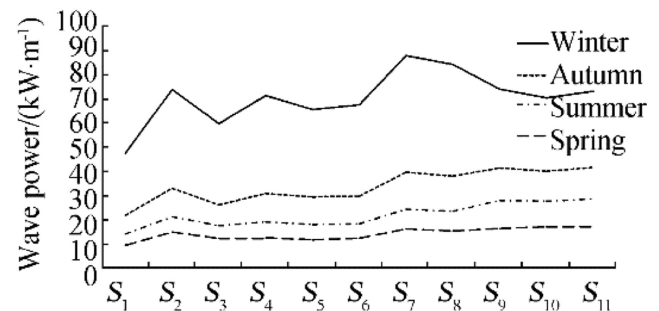
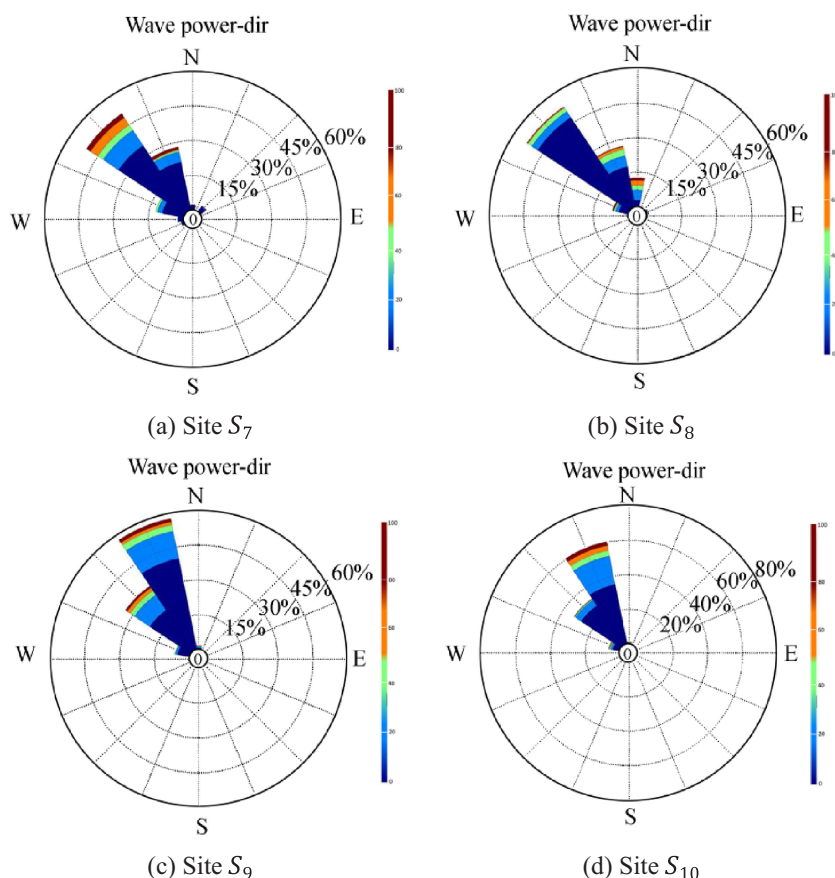


**Fig. 13** Seasonal mean values of wave power per unit crest length ( $\text{kW} \cdot \text{m}^{-1}$ )



**Fig. 14** Directional distribution of wave power



In order to determine the monthly variability, the index of Eq. (7) is used. In fact, small monthly variability index values indicate less variability in wave power. According to Table 2, the monthly variability index is decreasing passing from  $S_1$  to  $S_{11}$  with an increasing value noticed at  $S_{10}$ . Hence, the locations  $S_7$  to  $S_9$ , and  $S_{10}$  to  $S_{11}$  present a uniform temporal variability throughout the year (less than 1.5), and, therefore, are suitable sites for WECs deployment. The other sites  $S_1$  to

$S_6$  reveal variability index of more than 2 which means more fluctuating wave power.

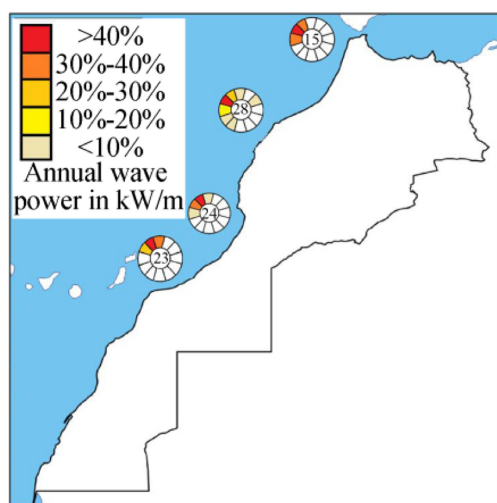
#### 4.4 Seasonal Variations in Wave Power

Figure 13 shows the average seasonal wave power for the 11 selected sites. As indicated, the wave energy in the Atlantic coast of Morocco shows a strong seasonal character, with significant variations between the seasons. For almost all the studied locations, the wave power in winter months is three times greater than in summer with values exceeding  $40 \text{ kW} \cdot \text{m}^{-1}$ . Uniform distribution of the seasonal mean wave power is expressed at the other seasons.

To analyze the seasonal temporal variability, the coefficient ( $S_v$ ) given by Eq. (6) was computed. As indicated in Table 2, the coefficient values are decreasing from sites with latitudes  $34^\circ \text{ N}$  to  $35^\circ 30' \text{ N}$  ( $S_1$  to  $S_3$ ) to sites with latitudes  $30^\circ 30' \text{ N}$  and  $33^\circ \text{ N}$  ( $S_{10}$  to  $S_{11}$ ). The sites  $S_7$  to  $S_{11}$  present less variability for  $S_v$  (from 1.10 and 1.34).

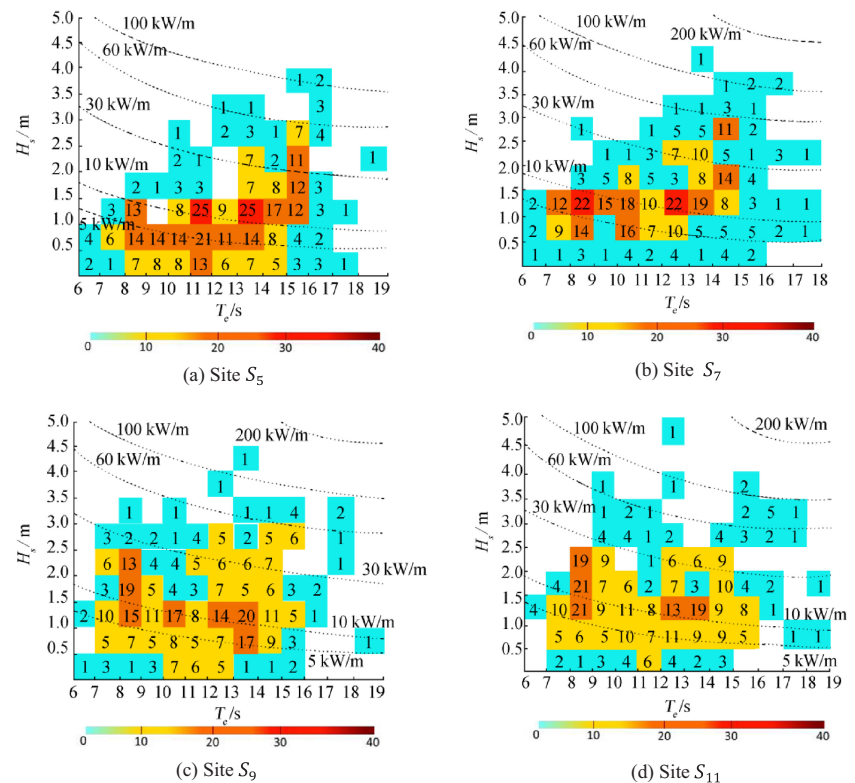
#### 4.5 The Energy-Rich Areas for WEC Deployment

Planning and operation of wave energy converters require a particular range of operating conditions in terms of wave height and period variations. Extensive researches on



**Fig. 15** Annual mean wave power roses for the most energetic sites

**Fig. 16** Bivariate distributions of occurrences corresponding to the sea states ( $H_s - T_e$ )



WECs indicate that these systems require at least  $20 \text{ kW} \cdot \text{m}^{-1}$  of annual mean wave power to be viable (Arinaga and Cheung 2012; Luiz et al. 2013). These values correspond to the moderate areas with higher latitudes. According to the results from the previous sections and Table 2, these areas are concentrated at the sites located between latitudes  $30^\circ 30' \text{ N}$  and  $33^\circ \text{ N}$  of the Atlantic coast of Morocco, where the temporal variabilities (monthly, seasonal) are shown to be more uniform and the annual mean wave power is of higher value.

Moreover, the difference between various WECs is their ability to direct themselves toward the incoming waves. This orientation could influence the amount of energy received by the WEC (Mota and Pinto 2014). The rose diagrams of wave power for the potential sites  $S_7$ ,  $S_8$ ,  $S_9$ , and  $S_{10}$  were plotted in Figs. 14 and 15 to highlight the sectors of higher incoming wave energy corresponding to NW and NNW.

As depicted in Fig. 16, occurrence analysis between  $H_s$  and  $T_e$  was conducted for a 3-year set of data records corresponding to four selected regions, with the wave power isolines. These figures indicate the ranges of  $H_s$  and  $T_e$  of the sea state that comprises significant wave power events. Such information could be useful for WECs deployment. It is shown that the most operational ranges are comprised between  $T_e$  10 to 14 s and  $H_s$  0.5 to 1.5 m at  $S_1$ , and between  $T_e$  9 to 14 s and  $H_s$  1 to 2.5 m at sites  $S_7$  to  $S_9$  (Fig. 16b, c). At the location  $S_{11}$ , the significant events are comprised between 8 to 9 s for  $T_e$  and 1 to 2.5 m for  $H_s$  (Fig. 16d).

## 5 Conclusion

The wave energy potential was evaluated for 11 sites along the Atlantic coast of Morocco in order to identify the suitable areas for WECs deployment. This analysis shows significant differences between the areas of the coast located between latitudes  $30^\circ 30' \text{ N}$  and  $33^\circ \text{ N}$  and the rest of the sites in terms of significant wave height and the resulting wave power. This wave energy resource is revealed to be more intense at sites between latitudes  $30^\circ 30' \text{ N}$  and  $33^\circ \text{ N}$  with an average annual wave power available of around  $30 \text{ kW} \cdot \text{m}^{-1}$ , while lower values are noticed for areas located between latitudes  $29^\circ \text{ N}$  to  $30^\circ \text{ N}$  and  $34^\circ \text{ N}$  to  $35^\circ 30' \text{ N}$ . Most of the energetic sites are concentrated at significant wave heights between 2 and 2.5 m, and wave period between 10 and 12 s. Regarding the incoming wave directions, sectors from N, NNW, and NW are the most energetic. The temporal variabilities along the Atlantic coast show a significant monthly variability with higher values in winter (January to March), and lower values in summer (June to August). Moreover, the seasonal variability is noticed to be of higher-energy in winter.

**Acknowledgments** This research work has been conducted as part of the research activity within the EMISys research team at the Turbomachinery Lab with the institution's financial support of Mohammadia School of Engineers and Mohammed V University in Rabat.

## References

- Abbaspour M, Rahimi R (2011) Iran atlas of offshore renewable energies. *Renewable Energy* 36:388–398. <https://doi.org/10.1016/j.renene.2011.06.051>
- Akpınar A, Kömürçü Mİ (2012) Wave energy potential along the south-east coasts of the Black Sea. *Energy* 42:289–302. <https://doi.org/10.1016/j.energy.2012.03.057>
- Angelis-Dimakis A, Markus B, Michela R, Dominguez J, Fiorese G, Gadocha S, Gnansounou E, Guariso G, Kartalidis A, Panichelli L, Pinedo I (2010) Methods and tools to evaluate the availability of renewable energy sources. *Renew Sust Energ Rev* 15(2):1182–1200. <https://doi.org/10.1016/j.rser.2010.09.049>
- Antonio F, Falcão O (2010) Wave energy utilization: a review of the technologies. *Renew Sust Energ Rev* 14:899–918. <https://doi.org/10.1016/j.rser.2009.11.003>
- Antonio F, Falcão O (2014) Modeling of wave energy conversion. Instituto Superior Técnico. Universidade Técnica de Lisboa, 160.
- Aparicio D (2014) ICEx: El Mercado de las energías renovables en Marruecos, Technical Report, ICEx. Ministerio de Economía y Competitividad, Madrid
- Arinaga RA, Cheung KF (2012) Atlas of global wave energy from 10 years of reanalysis and hindcast data. *Renew Energy* 39:49–64. <https://doi.org/10.1016/j.renene.2011.06.039>
- Booij N, Ris RC, Holthuijsen LH (1999) A third-generation wave model for coastal regions, part I, model description and validation. *J Geophys Res Oceans* 104(C4):764–966. <https://doi.org/10.1029/98JC02622>
- Cornett A (2008) A global wave energy resource assessment. Proceedings of the Eighteenth International Offshore and Polar Conference, 6–11
- Drew B, Plummer A, Sahinkaya M (2009) A review of wave energy converter technology. *P I Mech Eng A-J Pow* 223:887–902. <https://doi.org/10.1243/09576509JPE782>
- Duckers L (2004) Wave energy. In: Boyle G (ed) *Renewable energy*. 2nd ed. Oxford University Press, Oxford
- Ertekin RC, Yingfan X (1994) Preliminary assessment of the wave-energy resource using observed wave and wind data. *Energy* 19: 729–738. [https://doi.org/10.1016/0360-5442\(94\)90011-6](https://doi.org/10.1016/0360-5442(94)90011-6)
- Fadaeenejad M, Shamsipour R, Rokni SD, Gomes C (2014) New approaches in harnessing wave energy: with special attention to small islands. *Renew Sust Energ Rev* 29:345–354. <https://doi.org/10.1016/j.rser.2013.08.077>
- Falcão FO, Henriques JCC (2016) Oscillating-water-column wave energy converters and air turbines: a review. *Renew Energy* 85:1391–1424. <https://doi.org/10.1016/j.renene.2015.07.086>
- Gonçalves M, Martinho P, Soares CG (2014) Assessment of wave energy in the Canary Islands. *Renew Energy* 68:774–784. <https://doi.org/10.1016/j.renene.2014.03.017>
- Gunn K, Stock-Williams C (2012) Quantifying the global wave power resource. *Renew Energy* 44:296–304. <https://doi.org/10.1016/j.renene.2012.01.101>
- Hasselmann K, Hasselmann S, Bauer E, Janssen P, Komen G, Bertotti L, Lionello P, Guillaume A, Cardone V, Greenwood J, Reistad M, Zambresky L, Ewing J (1988) The WAM model – a third generation ocean wave prediction model. *J Phys Oceanogr* 18:1775–1810. [https://doi.org/10.1175/1520-0485\(1988\)018<1775:TWMTGO>2.0.CO;2](https://doi.org/10.1175/1520-0485(1988)018<1775:TWMTGO>2.0.CO;2)
- Holmbom J (2011) Modeling of waves and currents in the Baltic Sea. KTH, School of Architecture and the Built Environment, land and water resources engineering. Degree Project, 27.
- Iglesias G, Carballo R (2009) Wave energy potential along the Death Coast (Spain). *Energy* 34:1963–1975. <https://doi.org/10.1016/j.energy.2009.08.004>
- Iglesias G, Lopez M, Carballo R, Castro A, Fraguera JA, Frigaar P (2009) Wave energy potential in Galicia (NW Spain). *Renew Energy* 34: 2323–2333. <https://doi.org/10.1016/j.renene.2009.03.030>
- Iuppa C, Cavallaro L, Vicinanza D, Foti E (2015) Investigation of suitable sites for wave energy converters around Sicily (Italy). *Ocean Sci*, ISSN 1812-0784 11:543–557. <https://doi.org/10.5194/os-11-543-2015>
- Joubert JR (2008) An investigation of the wave energy resource on the South African coast, focusing on the spatial distribution of the south-west coast [M.S. thesis], University of Stellenbosch, Stellenbosch, South Africa
- Kamranzad B, Etemad-Shahidi A, Chegini V (2013) Assessment of wave energy variation in the Persian Gulf. *Ocean Eng* 70:72–80. <https://doi.org/10.1016/j.oceaneng.2013.05.027>
- Lewis A, Estefen S, Huckerby J, Musial W, Pontes T, Torres-Martinez J (2011) Ocean energy. In: IPCC special report on renewable energy sources and climate change. Cambridge University Press, Cambridge
- Liberti L, Carillo A, Sannino G (2013) Wave energy resource assessment in the Mediterranean, the Italian perspective. *Renew Energy* 50: 938–949. <https://doi.org/10.1016/j.renene.2012.08.023>
- López I, Andreu J, Ceballos S, Alegria IM, Kortabarria I (2013) Review of wave energy technologies and the necessary power-equipment. *Renew Sust Energ Rev* 27:413–434. <https://doi.org/10.1016/j.rser.2013.07.009>
- Luiz AO, Rocha LS, Bejan A (2013) Constructal law and the unifying principle of design. Springer, New York. <https://doi.org/10.1007/978-1-4614-5049-8>
- Mørk G, Barstow S, Kabuth A, Pontes MT (2010) Assessing the global wave energy potential. Proceedings of OMAE 2010, 29<sup>th</sup> International Conference on Ocean, Offshore Mechanics and Arctic Engineering, Shanghai, China. <https://doi.org/10.1115/OMAE2010-20473>
- Mota P, Pinto JP (2014) Wave energy potential along the western Portuguese coast. *Renew Energy* 71:8–17. <https://doi.org/10.1016/j.renene.2014.02.039>
- Pinet P (2006) Invitation to oceanography. Ph.D. thesis, Colgate University, 662
- Saket A, Etemad-Shahidi A (2012) Wave energy potential along the northern coasts of the Gulf of Oman. *Renew Energy* 40:90–97. <https://doi.org/10.1016/j.renene.2011.09.024>
- Sierra JP, González-Marco D, Sospedra J, Gironella X, Mösso C, Sánchez-Arcilla A (2013) Wave energy resource assessment in Lanzarote (Spain). *Renew Energy* 55:480–489. <https://doi.org/10.1016/j.renene.2013.01.004>
- Sierra JP, Martín C, Mosso C, Mestres M, Jebbad R (2016) Wave energy potential along the Atlantic coast of Morocco. *Renew Energy* 96: 20–32. <https://doi.org/10.1016/j.renene.2016.04.071>
- Stopa JE, Filipot JF, Li N, Cheung KF, Chen YL, Vega L (2013) Wave energy resources along the Hawaiian Island chain. *Renew Energy* 55:305–321. <https://doi.org/10.1016/j.renene.2012.12.030>
- Tolman HL, Bhavani B, Burroughs LD, Chalikov DV, Chao YY, Chen HS, Gerald VM (2002) Development and implementation of wind-generated ocean surface wave. Modelsat NCEP. [https://doi.org/10.1175/1520-0434\(2002\)017<0311:AIOWG>2.0.CO;2](https://doi.org/10.1175/1520-0434(2002)017<0311:AIOWG>2.0.CO;2)
- Vannucchi V, Cappietti L, Falcão AFO (2012) Estimation of offshore wave energy potential of the Mediterranean sea and propagation toward a nearshore area. 4th International Conference on Ocean Energy, Dublin
- Zodiatis G, Galanis G, Nikolaidis A, Kalogeris C, Hayes D, Georgiou GC, CChu P, George K (2014) Wave energy potential in the Eastern Mediterranean Levantine Basin. An integrated 10-year study. *Renew Energy* 69:311–323. <https://doi.org/10.1016/j.renene.2014.03.051>